Highly Efficient, Irreversible and Selective Ion Exchange Property of Layered Titanate Nanostructures

Nian Li, Lide Zhang, Yongzhou Chen, Ming Fang, Junxi Zhang, and Huimin Wang*

Layered titanates ($Na_2Ti_3O_7{\cdot}nH_2O$) with exchangeable sodium cations located in the interlayer have been synthesized by simple hydrothermal treatment of Ti precursor in concentrated NaOH solutions. By proper control of the synthesis conditions, different morphologies of nanofibers and nanosheets are obtained. The metastable layered structure of the titanates collapses during the ion exchange, resulting in irreversible ion exchange. Target cations (eg., Ag^+, Cu^{2+}, Pb^{2+} and Eu^{3+}) are completely concentrated from water and then tightly immobilized in the interlayer which is of great significance for the removal and subsequent safe disposal of hazardous metal cations. The ion exchange of the nanosheets is much more efficient than that of the nanofibers and other inorganic ion exchangers due to the larger surface area, less stable layered structure and larger amount of interlayer water of the nanosheets. The ion exchange of the titanates is also very selective. Valence, hardness, and radius of cations are main factors affecting the selectivity. Cations trapped in the interlayer are released by an acid-induced phase transformation of the titanate nanosheets to rutile. Then the rutile can be used as a new Ti precursor to synthesize the titanate nanostructures, resulting in a full cycle of material use. The nanosheets may find applications in the decontamination and safe disposal of radioactive and heavy metal cations and also in the collection of valuable cations from water.

1. Introduction

Ion exchange is regarded as a technology of great importance in many practical applications, such as the removal of toxic substances and the collection of valuable elements from water.[1–3] The searching and designing of efficient and economical ion exchangers have been extensively conducted, especially, for the decontamination of radioactive waste generated from nuclear accidents or uranium mining and for the recovery of heavy metals in wastewater.[4–22] In the nuclear industry, ion exchange is also an effective method to transfer the radioactive content of a large volume of liquid into a small volume of solid which can be placed in a given amount of repository space.[23] Organic resins are most commonly used ion exchangers for these purposes.[23] But during the past years, inorganic layered ion exchangers such as metal phosphates,[4] synthetic micas,[5–7] clay minerals,[8] magadiites[9] and titanates[13–21] have emerged as an increasingly important replacement or complement. These layered materials often have the advantages of much greater selectivity for target cations and higher resistibility to radiation and temperature compared with organic resins. Furthermore, for some metastable layered materials, a structure collapse occurs during the ion exchange, resulting in tight immoblization of target cations in the interlayer and thus the irreversible ion exchange.[4–7,20,21] This is of great significance for the complete concentration of target cations from water and the safe disposal of entrapped hazardous cations to avoid leaching from the ion exchangers.[4–7,20–22] In contrast, back exchange occurs readily in organic resins and other reversible ion exchangers. However, all these layered materials have certain drawbacks which limit their practical applications: a) a long contact time of several days or even more is always required to reach the sorbent–solution equilibrium; b) the interlayer ions can not be exchanged out completely, resulting in low exchange capacities; c) the recovery of entrapped cations and the regeneration of materials can hardly be achieved after the collapse of layered structure, which limits their applications in the collection of valuable cations and also leads to a waste of materials. Moreover, the mechanism of the ion exchange in layered materials and the factors affecting the efficiency and selectivity of the ion exchange need to be further investigated.

In the meantime, micro- and nanosized materials have played important roles in many areas, including catalysis,[24,25] optics,[26] electronics,[27] and environment.[28] Due to their unique physical and chemical properties, they may also offer the potential to design novel inorganic ion exchangers which can overcome the drawbacks mentioned above. In this study, we report the synthesis of layered titanate nanofibers and nanosheets with exchangeable sodium cations located in the interlayer. Although titanates have long been considered as possible ion exchangers,[13–21] the unique structure of the

N. Li, Prof. L. D. Zhang, Y. Z. Chen, Dr. M. Fang, Dr. J. X. Zhang, H. M. Wang
Key Laboratory of Materials Physics
Anhui Key laboratory of Nanomaterials and Nanostructure
Institute of Solid State Physics
Chinese Academy of Sciences, Hefei 230031, PR China
E-mail: ldzhang@issp.ac.cn

DOI: 10.1002/adfm.201102272

nanosheets makes it a new candidate with highly efficient, irreversible and selective ion exchange properties. Target cations are immobilized tightly in the interlayer after the exchange. By comparing the adsorption behaviour of the nanosheets and nanofibers, essential mechanism of the ion exchange as well as the selectivity is discovered. Moreover, the nanosheets after the ion exchange are 100% regenerated for possible metal collection through an acid-induced phase change. This can't be achieved in the nanofibers and other layered ion exchangers after the structure collapse.[4–7,20,21] In addition, the titanates are readily fabricated by a hydrothermal treatment of Ti precursors in concentrated NaOH solutions at moderate temperature. Various Ti precursors (rutile, anatase, and amorphous TiO_2) can be used to synthesize the titanates with close to 100% conversion efficiency.[29–33] Herein, industrial grade metatitanic acid (TiO_2•H_2O) is chosen as the Ti precursor which makes the synthesis very cost effective for industrial-scale applications.

2. Results and Discussion

Figure 1 shows typical SEM and TEM images of titanates synthesized at different NaOH concentrations. The growth of the nanostructures during the hydrothermal process follows 3D → 2D → 1D mechanism.[34] The raw Ti precursor is first transformed into 2D lamellar structures and then roll to form 1D structures. As shown in Figure 1a, nanofibers are formed at 10M NaOH. While at 5 M NaOH, the lamellar structures cannot roll into 1D structures due to the low concentration of base solution,[35] thus nanosheets are obtained (Figure 1b). The typical value of the BET specific surface area of the nanosheets is measured as 203 $m^2 \cdot g^{-1}$, which is much larger than the value of the nanofibers with S_{BET} = 37 $m^2 \cdot g^{-1}$. The difference of the surface area will significantly influence their ion exchange performance.

The powder XRD patterns of the nanofibers and nanosheets are shown in **Figure 2**. As can be seen, the main peaks of both are typical of layered titanates, especially the one at around $2\theta = 10°$, attributed to the interlayer distance in $Na_2Ti_3O_7$•nH_2O (JCPDs no. 72–0148).[36–39] In the titanates, three edge-shared TiO_6 octahedra join at the corner to form stepped $Ti_3O_7^{2-}$ layers, sodium ions and water molecules located between the layers are exchangeable. The interlayer distance d_{100} of the titanate nanosheets (labeled as Na-TNSs) is 0.978 nm which is larger than the value of the nanofibers (labeled as Na-TNFs) with d_{100} = 0.846 nm. This is due to the reason that there is more interlayer water in Na-TNSs than in Na-TNFs, as confirmed by the thermo gravimetric analysis (TGA, Figure S1 in the Supporting Information). Layered structures are metastable, less interlayer water makes Na-TNFs more stable than Na-TNSs. The inductively coupled plasma (ICP) spectroscopy is used to further confirm the chemical formula and obtain the accurate amount of interlayer water in Na-TNFs and Na-TNSs. The molar ratio of Na to Ti of both is measured to be around 2:3. The chemical formulas are calculated approximately to be $Na_2Ti_3O_7$•$2H_2O$ for Na-TNFs and $Na_2Ti_3O_7$•$6H_2O$ for Na-TNSs, respectively.

To examine the ion exchange properties of Na-TNSs and Na-TNFs, several metal cations (M^{n+} = Ag^+, Pb^{2+}, Cu^{2+} and Eu^{3+}) are used. Among them, Ag^+ is a noble metal cation, Pb^{2+} and

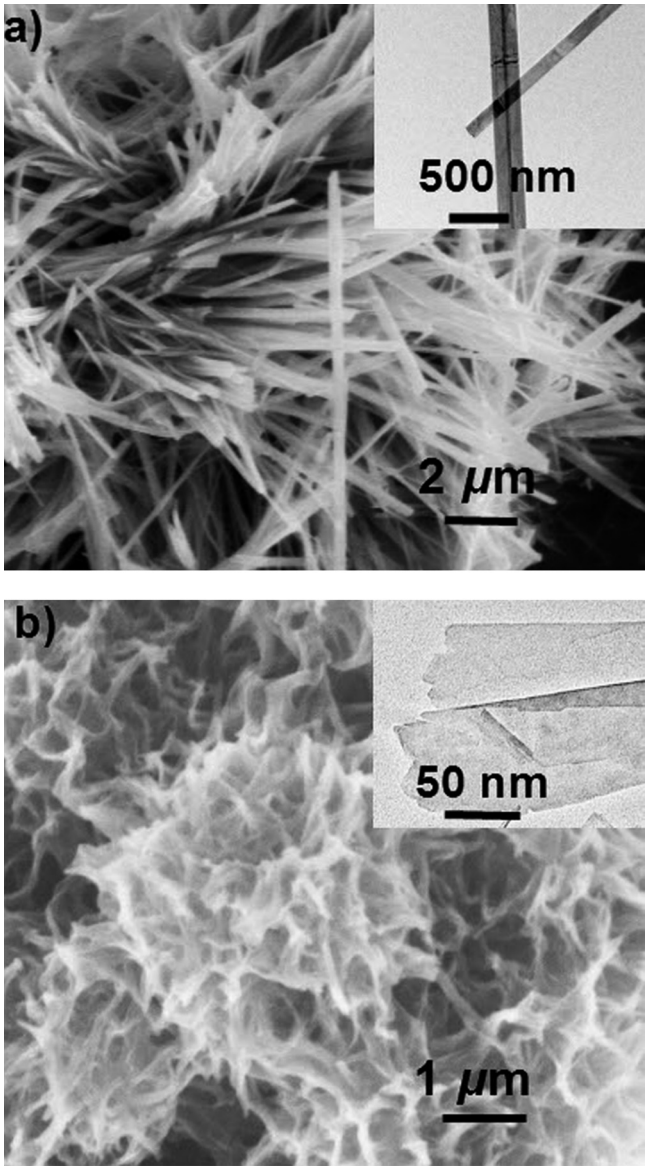

Figure 1. SEM images and low-resolution TEM images (inset) of titanates synthesized at a) 10 M and b) 5 M NaOH.

Cu^{2+} are common heavy metal contaminants, and Eu^{3+} is a trivalent lanthanide and a chemical homologue to trivalent radioactive actinides with the similar sorption and ion exchange properties.[40,41] Thus, Eu^{3+} is used as a representative of ultratoxic radioactive actinides. The pH values of metal solutions before and after the ion exchange are also measured (Table S1 in the Supporting Information). No precipitation of cations is observed in the whole process. The XRD patterns of the samples after the metal uptake are shown in Figure 2. The collapse of the layered structure caused by the ion exchange can be seen from the shift of d_{100} peak. For Na-TNFs, the residual peak at 0.846 nm in each sample indicates that the exchange of Na^+ is not completed (Figure 2a). The exchange of Cu^{2+} is most efficient as revealed by the weakest residual peak intensity. In contrast, the exchange of Ag^+ has the lowest efficiency and the

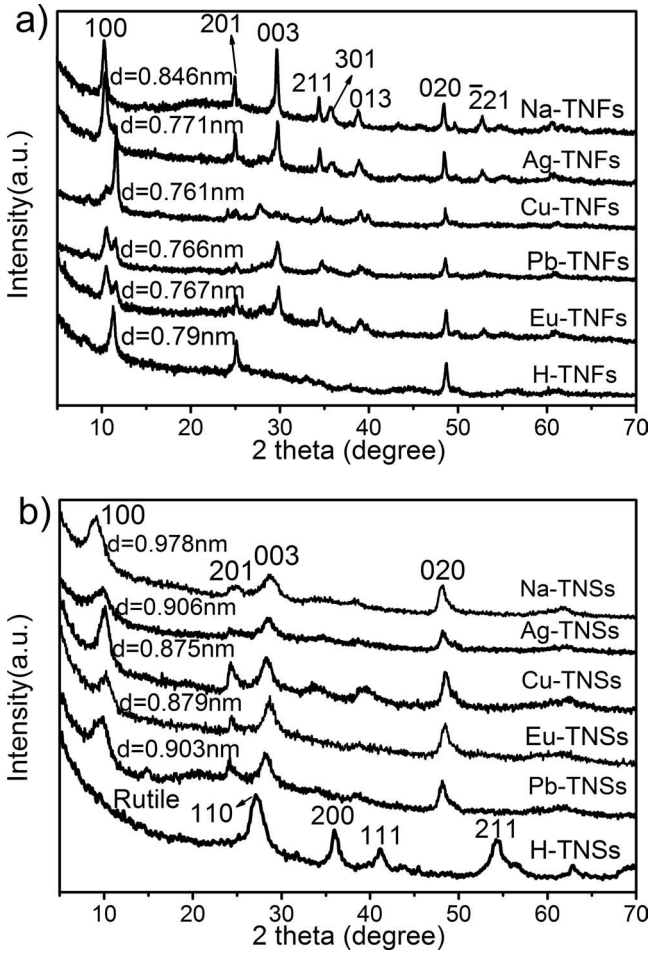

Figure 2. XRD patterns of a) Na-TNFs and b) Na-TNSs before and after the ion exchange with M^{n+} and H^+ (M^{n+} =Ag^+, Cu^{2+}, Pb^{2+}, and Eu^{3+})

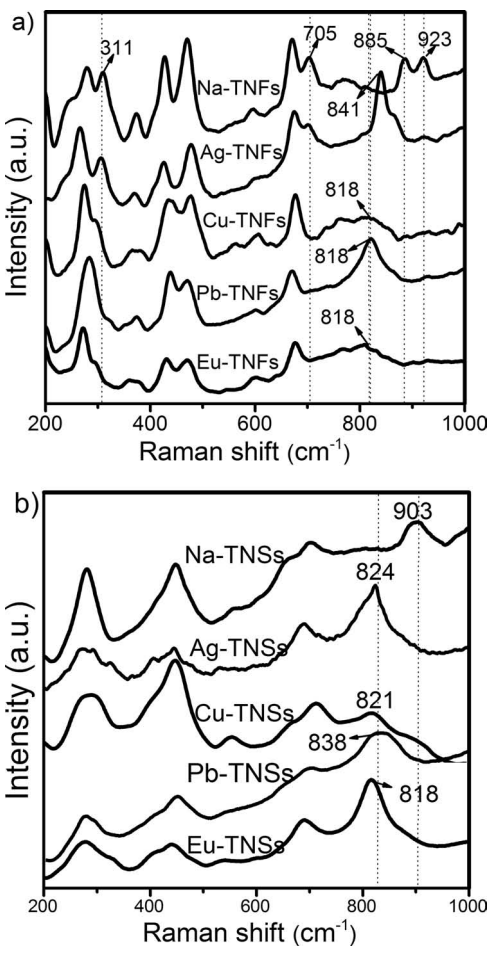

Figure 3. Raman spectra of a) Na-TNFs and b) Na-TNSs before and after the ion exchange.

reason will be discussed later. While for Na-TNSs, all Na^+ cations are completely exchanged in each sample and a remarkable decrease of the interlayer distance between 0.07–0.1 nm is observed (Figure 2b). This is due to the less stable structure, more interlayer water and larger surface area of Na-TNSs than Na-TNFs. These results are consistent with the energy-dispersive x-ray (EDX, Figure S2 in the Supporting Information) and ICP analysis of the samples before and after the ion exchange. The complete exchange of Na^+ in Na-TNSs implies that Na-TNSs have a much larger adsorption capacity than Na-TNFs and other layered ion exchangers (eg., metal phosphates, synthetic micas, clay minerals, and magadiites) in which complete exchange of interlayer ions cannot be achieved.[4–9]

Raman spectra of the samples before and after the ion exchange are shown in **Figure 3**. For Na-TNFs in Figure 3a, the spectra are essentially the same as the data reported for layered tri-titanates.[33,42–44] And for Na-TNSs in Figure 3b, the spectra are the same as the report for tri-titanates synthesized at relatively lower temperature or lower NaOH concentration.[45–48] The peak near 903 cm^{-1} in Na-TNSs is attributed to the short Ti–O stretching vibration involving nonbridging oxygen atoms (in disordered TiO_6 octahedron) that are coordinated with Na^+. As Na^+ is exchanged, this peak shifts to lower frequencies. The new peaks are assigned to the short Ti-O vibration affected by M^{n+}. In Na-TNFs, the peaks near 311 cm^{-1} and 705 cm^{-1} correspond to the Ti–O–Na vibration. The two peaks just disappear after the exchange of Na^+ by Cu^{2+}, Pb^{2+} and Eu^{3+}. While in Ag-TNFs, these peaks still exist but in a lower intensity due to the reason that few Na^+ ions are exchanged by Ag^+, which is consistent with the above XRD analysis. The peak of short Ti–O vibration coordinated with Na^+ is at 885 $cm^{-1}$and 923 cm^{-1} in Na-TNFs. And this peak shifts to lower frequencies after the ion exchange just like in Na-TNSs.

Figure 4 shows the Fourier Transform Infrared Spectra (FTIR) of samples before and after the ion exchange. The spectra in Figure 4a and 4b are similar to the data reported for layered tri-titanates.[43,44,47,49] The peaks at 881 cm^{-1} in Figure 4a and 908 cm^{-1} in Figure 4b are assigned to the stretching vibration of short Ti-O bonds from disordered TiO_6 octahedron whose oxygen is unshared. This stretching is affected by interlayer ions. The spectra of samples after the ion exchange in the region between 1200 cm^{-1} and 400 cm^{-1} are shown in Figure 4c and Figure 4d. For Na-TNSs in Figure 4c, the peak at 881 cm^{-1} is disappeared in Cu-, Pb-, Eu- and H-TNSs, but still exists in

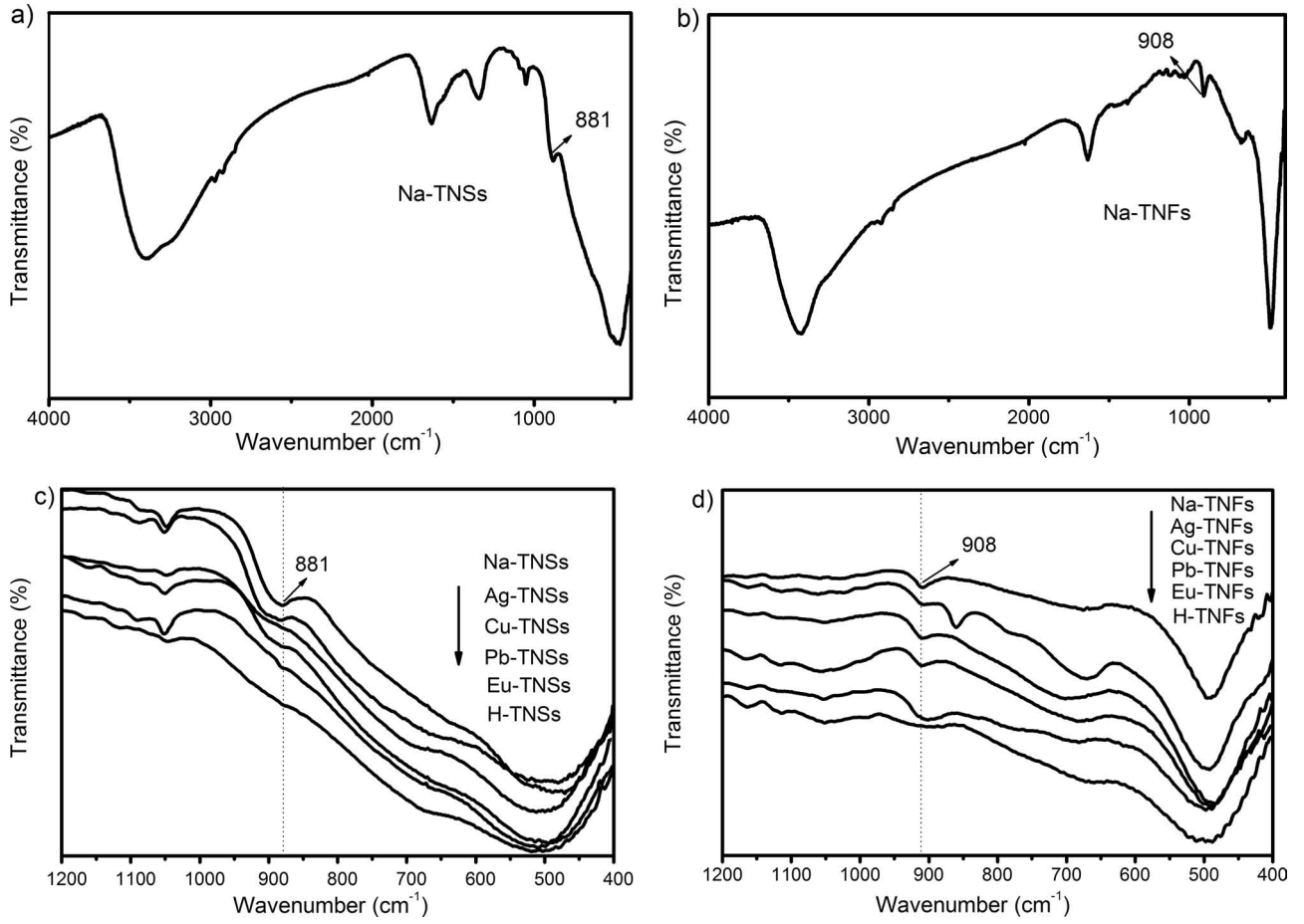

Figure 4. a,b) FTIR spectra of a) Na-TNSs and b) Na-TNFs in the region between 4000 cm^{-1} and 400 cm^{-1}. c,d) FTIR spectra of c) Na-TNSs and d) Na-TNFs before and after the exchange of Na^+ by M^{n+} and H^+ in the region between 1200 cm^{-1} and 400 cm^{-1}.

Ag-TNSs. We suppose it is caused by the reason that the distribution of monovalent Ag^+ in the interlayer is similar to Na^+. Thus, Ag^+ may has the similar affect on the Ti-O vibration as Na^+. For Na-TNFs in Figure 4d, the peak at 908 cm^{-1} doesn't change much after the ion exchange except in H-TNFs due to large amount of remaining Na^+ in the interlayer. The new peak at 860 cm^{-1} in Ag-TNFs can't be explained for sure.

The collapse of the layered structure immobilizes M^{n+} inside the interlayer, resulting in irreversible ion exchange. To verify the tightness of the immobilization which is very important in the subsequent safe disposal, Cu-TNSs were first rinsed to remove surface adsorbed Cu^{2+} and then mixed with a solution with excess amount of aqueous hydrazine (which could easily reduce Cu^{2+} to Cu^0). No red elemental copper was formed in the solution, even after tens of hours of hydrothermal treatment at 120 °C. This indicates that Cu^{2+} was tightly bound into the interlayer, and therefore was prevented from being reduced by aqueous hydrazine. As a result, hazardous cations (eg., radioactive cations) trapped in the titanates can be safely disposed of with no worry of leaching.

The theoretical cation exchange capacities (CECs) of Na-TNFs and Na-TNSs are calculated from their chemical formulas to be 5.91 and 4.88 meq·g^{-1}, respectively. **Figure 5**a and 5b show the adsorption isotherms of M^{n+} on Na-TNFs and Na-TNSs, respectively. Each isotherm follows Langmuir model well (Table S2 in the Supporting Information).[50] For Na-TNFs, the maximum adsorption capacities are lower than the theoretical CEC due to the incomplete exchange of Na^+ by M^{n+}. For Na-TNSs, the maximum adsorption capacities are 5.06 meq·g^{-1} for Ag^+, 6.42 meq·g^{-1} for Cu^{2+}, 5.44 meq·g^{-1} for Pb^{2+}, and 5.21 meq·g^{-1} for Eu^{3+}. The part exceeding the theoretic CEC is attributed to the adsorption at the large negatively charged surface after the ion exchange is saturated. This adsorption capacity of Na-TNSs is much larger than other adsorbents (eg., metal phosphate, synthetic mica, clay minerals, and magadiite) which have capacities in the range of 0.5–2.0 meq·g^{-1}.[4–9]

The adsorption kinetic curves of M^{n+} on Na-TNFs and Na-TNSs are shown in Figure 5c and 5d, respectively. For Na-TNFs, the adsorption is completed within 24–48 h. For Na-TNSs, the adsorption is extremely prompt. The time needed for complete removal of Cu^{2+} is just 30 min and 86% Cu^{2+} ions are adsorbed in the first 5 min. The adsorption of Ag^+, Pb^{2+}, and Eu^{3+} is also completed within 60–120 min. In comparison, Sr^{2+} absorption on Na-4-mica and Zn^{2+} adsorption on magadiite take 28 days and 1 day, respectively.[7,9] It is also worth emphasizing that the efficiency of M^{n+} adsorption on Na-TNSs is almost 100%. The residual concentration of M^{n+} after the adsorption is at the level

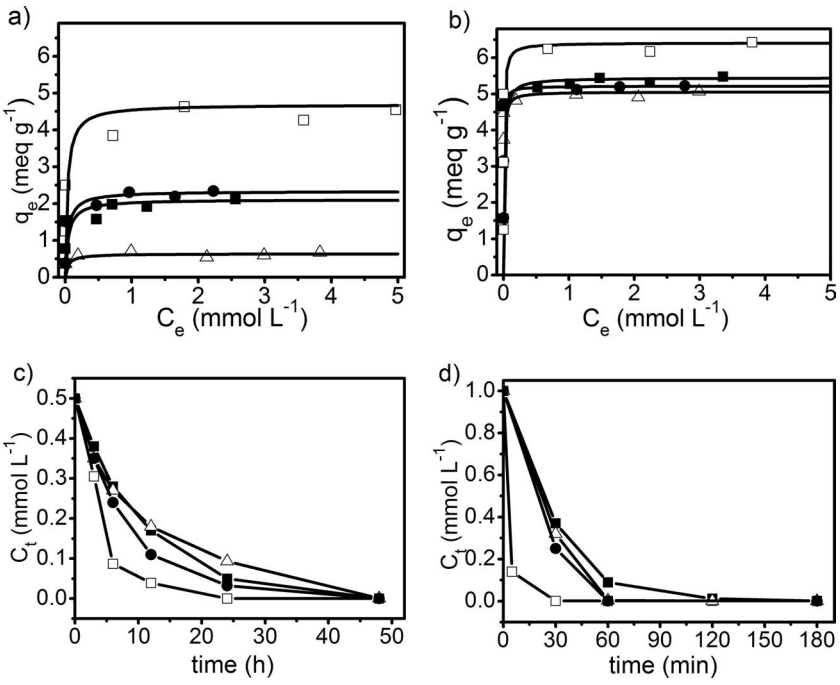

Figure 5. a,b) Adsorption isotherms of M^{n+} on a) Na-TNFs and b) Na-TNSs. c,d) Adsorption kinetic curves of M^{n+} on c) Na-TNFs and d) Na-TNSs. M^{n+} = (Δ) Ag^+, (□) Cu^{2+}, (■) Pb^{2+} and (●) Eu^{3+}, C_e = equilibrium concentration, q_e = adsorbed amount, C_t = concentration at time t.

of 10^{-5}–10^{-4} mmol·L^{-1} which is under the standards for heavy metals in drinking water recommended by the World Health Organization (WHO).[51] The complete removal is also the benefit of the irreversible ion exchange which prevents release of M^{n+} to the solution. The high adsorption capacity, prompt speed and complete removal fully demonstrate that the ion exchange of Na-TNSs is highly efficient.

In addition to Cu^{2+}, Pb^{2+} and Eu^{3+} mentioned above, we have also studied the ion exchange of many other multivalent caions, such as Sr^{2+}, Ba^{2+}, Zn^{2+}, Cd^{2+}, Fe^{2+}, Fe^{3+}, Cr^{3+}, Ni^{3+}, Mg^{2+}, and Ca^{2+}. It is found that the intercalation of all these cations into Na-TNSs is completed. Due to the stoichiometric nature of the ion exchange, the replacement of monovalent Na^+ by multivalent M^{n+} ($n \geq 2$) decreases the number of ions in the interlayer. This will lead to a shrinking of the basal spacing and then the layered structure becomes more stable. As a result, all multivalent cations can be adsorbed by Na-TNSs efficiently and the cation with higher valence is more preferred in the ion exchange.

The complete intercalation of monovalent Ag^+ into Na-TNSs is guided by another mechanism. According to Pearson's Hard-Soft Acid-Base (HSAB) Principal, hard acids bind strongly to hard bases and soft acids bind strongly to soft bases.[52–56] Metal cations in solution serve as lewis acid. Based on their hardness value, they are classed as three groups: hard (eg., H^+, Li^+, Na^+ and K^+), soft (eg., Ag^+, Pd^{2+} and Au^+) and borderline (eg., Cu^{2+}, Pb^{2+} and Ni^{2+}). As a hard base, H_2O binds tightly to Na^+ in the interlayer of titanates. The exchange of Na^+ by soft acid (eg., Ag^+) is always accompanied by dehydration which also leads to the collapse of the layered structure. Thus, little water exists in Ag-TNSs and Ag-TNFs (Figure S1 in the Supporting Information) and Ag^+ adsorption on Na-TNFs with little interlayer water is inefficient. As a result, the interlayer of titanates prefers soft cations and the hardness of cations is another important factor affecting the ion exchange. To further confirm this, we have studied the ion exchange of Li^+ and K^+ by Na-TNSs (Figure S3 in the Supporting Information). Li^+ and K^+ are hard lewis acid just like Na^+. It is not surprising to find that the exchange of K^+ is not favourable, only 37.4% Na^+ ions are replaced. The exchange of Na^+ by Li^+ is completed due to the smaller radius of Li^+ which implies that the cation radius is also an important parameter. That's why the adsorption of Cu^{2+} is more efficient than Pb^{2+} as shown in Figure 5.

From the above discussion, there are three factors affecting the ion exchange. The cation with higher valence, lower hardness and smaller radius will be more preferred. **Table 1** shows the hardness, valence and radius values of some come cations.[52–57] The possibility and selectivity of the ion exchange can be predicted by comparing these values of two cations. In actual applications, there are always many competing cations coexisting with the target cations. For example, hard cations Na^+, Mg^{2+} and Ca^{2+} are usually present in contaminated wastewater at greater levels, resulting in the inefficiency of traditional treatment technology.[58] As shown in Table 1, Ag^+, Cu^{2+} and Pb^{2+} are much softer than Na^+, Mg^{2+} and Ca^{2+}, thus possess higher priority in the ion exchange. For Eu^{3+}, the hardness value was not presented by Pearson. But due to the similar chemical and physical properties with La^{3+}, Eu^{3+} may has the similar hardness value and be softer than Na^+, Mg^{2+} and Ca^{2+}. Compounded by the higher valence, Eu^{3+} is more preffered in the ion exchange. To confirm this, we have studied the adsorption of Ag^+, Cu^{2+}, Pb^{2+} and Eu^{3+} (1 mmol·L^{-1}) by Na-TNSs under the presence of large amount of Na^+, Mg^{2+} and Ca^{2+} (200 mmol·L^{-1}). Ag^+, Cu^{2+}, Pb^{2+} and Eu^{3+} are removed completely due to their higher priority against these hard cations. We also try to use Mg-TNSs and Ca-TNSs as ion exchangers to adsorb Ag^+, Cu^{2+}, Pb^{2+} and Eu^{3+}. Results show that the ion exchange is still very efficient and all Mg^{2+} and Ca^{2+} are replaced. All these reveal the super selectivity of the ion exchange.

H^+ (1 mol·L^{-1}) is used to regenerate the titanates due to the fact that H^+ is the smallest cation and thus may possess the highest priority in the ion exchange. From Figure 2a, we can see that the interlayer distance of H-TNFs is 0.79 nm which is exactly the value reported in $H_2Ti_3O_7$.[59] But ICP analysis shows that there is still 7.46 wt% of Pb^{2+} remaining in H^+ treated Pb-TNFs. For Na-TNSs, the layered structure is less stable and a phase change to rutile occurs which is of benefit to the complete metal separation (Figure 2b).[60] See Figure S4 in the Supporting Information for more details of the phase change. No Pb^{2+} is detected in H^+ treated Pb-TNSs. Then the metal is collected and the rutile is used as a new Ti precursor to synthesize the titanates. This leads to a whole cycle as shown in **Figure 6**.

Table 1. The values of absolute hardness and radius of some common cations.

Cations	Absolute hardness[a)]	Radius[b)] (Å)
H^+	∞ (hard)	–0.18
Li^+	35.1 (hard)	0.76
Na^+	21.1 (hard)	1.02
K^+	13.6 (hard)	1.38
Ag^+	6.9 (soft)	1.15
Rb^+	11.7 (hard)	1.52
Au^+	5.7 (soft)	1.37
Mg^{2+}	32.5 (hard)	0.72
Ca^{2+}	19.7 (hard)	1
Mn^{2+}	9.3 (hard)	0.83
Fe^{2+}	7.3 (borderline)	0.78
Ni^{2+}	8.5 (borderline)	0.69
Cu^{2+}	8.3 (borderline)	0.73
Hg^{2+}	7.7 (soft)	1.02
Sr^{2+}	16.3 (hard)	1.18
Pb^{2+}	8.5 (borderline)	1.19
Ba^{2+}	12.8 (hard)	1.38
Pd^{2+}	6.8 (soft)	0.86
Al^{3+}	45.8 (hard)	0.535
Sc^{3+}	24.6 (hard)	0.745
Fe^{3+}	13.1 (hard)	0.645
La^{3+}	15.4 (hard)	1.032
Eu^{3+}	–	0.947

[a)]The adsolute hardness values are taken from the literature by Pearson et al.;[52–56]
[b)]The data of cation radius is given by R. D. Shannon.[57]

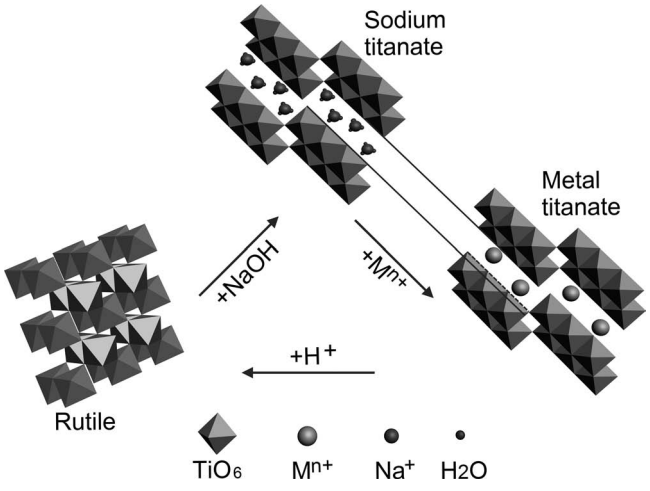

Figure 6. Schematic diagram of the ion exchange induced structure collapse as well as the regeneration of the titanates.

The efficiency of each step in this cycle is nearly 100% which reveals the great application prospect of Na-TNSs as an excellent ion exchanger. They can not only be used in the decontamination and safe disposal of radioactive and heavy metal cations, but also in other applications, such as the collection of noble metal cations (eg., Pd^{2+}, Pt^{4+}, Au^+ and Au^{3+}) and the softening of hard water (removal of Mg^{2+} and Ca^{2+}).

3. Conclusions

In summary, we have reported the highly efficient, irreversible and selective ion exchange property of titanate nanosheets caused by the unstable layered structure, large amount of interlayer water and large surface area. The valence, hardness and radius of cations are main factors determining the possibility and selectivity of the ion exchange. Target cations are completely concentrated from water and then tightly immobilized in the interlayer. An acid-induced phase change to rutile leads to the separation of entrapped metal cations and then the regeneration of the titanates. These findings offer important experimental basis for the understanding and searching of ion exchangers for target ions.

4. Experimental Section

Synthesis: Metatitanic acid (3g, industrial grade, purchased from Shanghai Mintchem Development Co., Ltd.) were mixed with 5 M or 10 M NaOH solutions (40 ml) and hydrothermal treated at 200 °C for 30 h. After the reaction, the precipitate was separated and washed with water until pH 12 and then rinsed with ethanol to remove the residual surface OH^- and Na^+. Finally, the samples were dried at 80 °C overnight.

Ion Exchange: Titanates (50 mg) were allowed to react with nitrate or chloride metal solutions (40 ml) with a desired concentration at room temperature. After a given time, the titanates were separated and the remaining metal concentration in the supernatants was measured. All experiments were duplicated and only mean values were reported.

Regeneration: The titanates after the metal uptake were treated by 1M HCl or HNO_3 and then separated and used as new Ti precursors to synthesize the titanates.

Chemical Composition Analysis: The chemical composition of the samples before and after the ion exchange was examined by both EDX and ICP methods. For ICP analysis, the samples were first dried for 4 h at 80 °C to remove the surface adsorbed water, then immediately weighed and dissolved by concentrated HNO_3. The solution was diluted and sent for ICP measurement. The chemical composition was calculated from the ICP results. To obtain the accurate chemical formulas of Na-TNSs and Na-TNFs, this measurement was carried out for 3 times, and mean values were reported.

Surface Charge of The Titanates: Zeta potential of the Na-TNSs is measured using the ZetaMeter (zetasizer 3000HSA, Malvern). The point of zero charge (PZC) is measured to be around pH 3.0. At pH>3, the surface is negatively charged. The electrostatic force between the surface and the cations is of benefit to the ion exchange and some cations can be adsorbed on the surface after the ion exchange was saturated.

Characterization: X-ray diffraction (XRD) analyses were performed on a powder diffractometer (X'Pert Pro MPD) with Cu Kα (λ = 1.5406 Å) radiation. The morphology of the samples was examined by field emission scanning electron microscopy (FESEM, FEI Sirion-200) and transmission electron microscope (TEM, JEM-2010). An energy dispersive x-ray spectrometer (EDX, Inca Oxford) in conjunction with the FESEM was used to examine chemical composition. Metal concentrations were measured by inductively coupled plasma spectrometer (ICP, Thermo

Scientific iCAP 6000). The detection limit was at the range of 10^{-5} mmol/L for most cations with proper detection wavelength. Vibrational property of samples was studied by Fourier transform infrared spectroscopy (FTIR, NEXUS) and Raman spectroscopy (Renishaw, inVia). Thermal gravimetric analysis (Pyris 1 TGA, Perkin-Elmer) was used to analyze the water content. Surface area and pore size distributions were measured using nitrogen as sorbate at 77K in a static volumetric apparatus (Tristar II 3020 M, Micromeritics).

Supporting Information

Supporting Information is available from the Wiley Online Library or from the author.

Acknowledgements

This work is supported by the National Basic Research Program of China (grant no. 2007CB936601). We thank Prof. Xiangke Wang at Institute of Plasma Physics, Chinese Academy of Sciences for helpful discussions.

Received: September 23, 2011
Published online: December 8, 2011

[1] A. A. Zagorodni, *Ion Exchange Materials: Properties and Applications*, Elsevier, Amsterdam, **2006**.
[2] A. M. Wachinski, J. E. Etzel, *Environmental Ion Exchange: Principles and Design*, CRC Press, Cleveland, OH, **1997**.
[3] B. A. Moyer, *Ion Exchange and Solvent Extraction: A Series of Advances, Volume 19*, CRC Press, Boca Raton, **2009**.
[4] S. Komarneni, R. Roy, *Nature* **1982**, *299*, 707.
[5] S. Komarneni, R. Roy, *Science* **1988**, *239*, 1286.
[6] S. Komarneni, N. Kozai, W. J. Paulus, *Nature* **2001**, *410*, 771.
[7] W. J. Paulus, S. Komarneni, R. Roy, *Nature* **1992**, *357*, 571.
[8] S. A. Adeleye, P. G. Clay, M. O. A. Oladipo, *J. Mater. Sci.* **1994**, *29*, 954.
[9] Y. Ide, N. Ochi, M. Ogawa, *Angew. Chem.* **2011**, *123*, 680; *Angew. Chem. Int. Ed.* **2011**, *50*, 654.
[10] C. Brenan, J. Lovatt, H. Smith, *Nature.* **1966**, *221*, 68.
[11] N. Ding, M. G. Kanatzidis, *Nat. Chem.* **2010**, *2*, 187.
[12] A. Dyer, M. Pillinger, J. Newton, R. Harjula, T. Moller, S. Amin, *Chem. Mater.* **2000**, *12*, 3798.
[13] J. Lehto, A. Clearfield, *J. Radioanal. Nucl. Chem. Lett.* **1987**, *118*, 1.
[14] A. Clearfield, J. Lehto, *J. Solid State Chem.* **1988**, *73*, 98.
[15] A. J. Celestian, D. G. Medvedev, A. Tripathi, J. B. Parise, A. Clearfield, *Nucl. Instrum. Methods Phys. Res. Sect. B* **2005**, *238*, 61.
[16] M. Nyman, D. T. Hobbs, *Chem. Mater.* **2006**, *18*, 6425.
[17] M. Poojary, R. A. Cahill, A. Clearfield, *Chem. Mater.* **1994**, *6*, 2364.
[18] A. J. Celestian, D. G. Medvedev, A. Tripathi, J. B. Parise, A. Clearfield, *J. Am. Chem. Soc.* **2008**, *130*, 11689.
[19] J. Lehto, R. Harjula, A. M. Girard, *J. Chem. Soc. Dalton Trans.* **1989**, *1*, 101.
[20] D. J. Yang, Z. F. Zheng, H. Y. Zhu, H. W. Liu, X. P. Gao, *Adv. Mater.* **2008**, *20*, 2777.
[21] D. J. Yang, Z. F. Zheng, H. W. Liu, H. Y. Zhu, X. B. Ke, Y. Xu, D. Wu, Y. Sun, *J. Phys. Chem. C* **2008**, *112*, 16275.
[22] G. L. Hill, E. Bailey, M. C. Stennett, N. C. Hyatt, E. M. Maddrell, P. F. McMillan, J. A. Hriljac, *J. Am. Chem. Soc.* **2011**, *133*, 13883.
[23] International Atomic Energy Agency (IAEA), Technical Reports Series No 408, Applications of Ion Exchange Process for the Treatment of Radioactive Waste and Management of Spent Ion Exchangers, Vienna, **2002**.
[24] J. Zeng, Q. Zhang, J. Y. Chen, Y. N. Xia, *Nano Lett.* **2010**, *10*, 30.
[25] M. C. Daniel, D. Astruc, *Chem. Rev.* **2004**, *104*, 293.
[26] J. Wang, M. S. Gudiksen, M. X. Duan, Y. Cui, C. M. Lieber, *Science* **2001**, *293*, 1455.
[27] A. J. Baca, J. H. Ahn, Y. G. Sun, M. A. Meitl, E. Menard, H. S. Kim, W. M. Choi, D. H. Kim, Y. Huang, J. A. Rogers, *Angew. Chem.* **2008**, *120*, 5606; *Angew. Chem. Int. Ed.* **2008**, *47*, 5524.
[28] L. D. Zhang, M. Fang, *Nano Today* **2010**, *5*, 128.
[29] T. Kasuga, M. Hiramatsu, A. Hoson, T. Sekino, K. Niihara, *Langmuir* **1998**, *14*, 3160.
[30] T. Kasuga, M. Hiramatsu, A. Hoson, T. Sekino, K. Niihara, *Adv. Mater.* **1999**, *11*, 1307.
[31] D. V. Bavykin, J. M. Friedrich, F. C. Walsh, *Adv. Mater.* **2006**, *18*, 2807.
[32] M. Grandcolas, A. Louvet, N. Keller, V. Keller, *Angew. Chem.* **2008**, *121*, 167; *Angew. Chem. Int. Ed.* **2008**, *48*, 161.
[33] A. Riss, T. Berger, S. Stankic, J. Bernardi, E. Knozinger, O. Diwald, *Angew. Chem.* **2008**, *120*, 1518; *Angew. Chem. Int. Ed.* **2008**, *47*, 1496.
[34] Y. Q. Wang, G. Q. Hu, X. F. Duan, H. L. Sun, Q. K. Xue, *Chem. Phys. Lett.* **2002**, *365*, 427.
[35] Y. F. Chen, C. Y. Lee, M. Y. Yeng, H. T. Chiu, *Mater. Chem. Phys.* **2003**, *81*, 39.
[36] Q. Chen, G. H. Du, S. Zhang, L. M. Peng, *Acta Crystallogr., Sect. B: Struct. Sci.* **2002**, *58*, 587.
[37] Y. V. Kolen'ko, K. A. Kovnir, A. I. Gavrilov, A. V. Garshev, J. Frantti, O. I. Lebedev, B. R. Churagulov, G. Van Tendeloo, M. Yoshimura, *J. Phys. Chem. B.* **2006**, *110*, 4030.
[38] M. Mori, Y. Kumagai, K. Matsunaga, I. Tanaka, *Phys. Rev. B* **2009**, *79*, 144117.
[39] E. Morgado, M. A. S. de Abreu, O. R. C. Pravia, B. A. Marinkovic, P. M. Jardim, F. C. Rizzo, A. S. Araujo, *Solid State Sci.* **2006**, *8*, 888.
[40] X. L. Tan, Q. H. Fan, X. K. Wang, B. Grambow, *Environ. Sci. Technol.* **2009**, *43*, 3115.
[41] N. Janot, M. F. Benedetti, P. E. Reiller, *Environ. Sci. Technol.* **2011**, *45*, 3224.
[42] A. Gajovic, I. Friscic, M. Plodinec, D. Ivekovic, *J. Mol. Struct.* **2009**, *924–926*, 183.
[43] X. M. Sun, Y. D. Li, *Chem. Eur. J.* **2003**, *9*, 2229.
[44] S. Papp, L. Korosi, V. Meynen, P. Cool, E. F. Vansant, I. Dekany, *J. Solid State Chem.* **2005**, *178*, 1614.
[45] Y. V. Kolenko, K. A. Kovnir, A. I. Gavrilov, A. V. Garshev, J. Frantti, O. I. Lebedev, B. R. Churangulov, G. V. Tendeloo, M. Yoshimura, *J. Phys. Chem. B* **2006**, *110*, 4030.
[46] X. D. Meng, D. Z. Wang, J. H. Liu, S. Y. Zhang, *Mater. Res. Bull.* **2004**, *39*, 2163.
[47] B. C. Viana, O. P. Ferreira, A. G. S. Filho, J. M. Filho, O. L. Alves, *J. Braz. Chem. Soc.* **2009**, *20*, 167.
[48] Y. Su, M. L. Balmer, *J. Phys. Chem. B* **2000**, *104*, 8160.
[49] O. P. Ferreira, A. G. S. Filho, J. M. Filho, O. L. Alves, *J. Braz. Chem. Soc.* **2006**, *17*, 393.
[50] R. I. Masel, *Principles of Adsorption and Reaction on Solid Surfaces*, John Wiley & Sons, New York **1996**.
[51] World Health Organization (WHO), *Guideline for Drinking-Water Quality:Recommendations*, 3rd ed., Geneva **2004**.
[52] R. G. Pearson, *J. Am. Chem. Soc.* **1963**, *85*, 3533.
[53] R. G. Pearson, *J. Chem. Educ. Ion.* **1968**, *45*, 581.
[54] R. G. Pearson, *J. Chem. Educ. Ion.* **1968**, *45*, 643.
[55] R. G. Parr, R. G. Pearson, *J. Am. Chem. Soc.* **1983**, *105*, 7512.
[56] R. G. Pearson, *Inorg. Chem.* **1988**, *27*, 734.
[57] R. D. Shannon, *Acta Cryst.* **1976**, *A32*, 751.
[58] B. J. Pan, H. Qiu, B. C. Pan, G. Z. Nie, L. L. Xiao, L. Lv, W. M. Zhang, Q. X. Zhang, S. R. Zheng, *Water Res.* **2010**, *44*, 815.
[59] Y. Suzuki, S. Yoshikawa, *J. Mater. Res.* **2004**, *19*, 982.
[60] H. Y. Zhu, Y. Lan, X. P. Gao, S. P. Ringer, Z. F. Zheng, D. Y. Song, J. C. Zhao, *J. Am. Chem. Soc.* **2005**, *127*, 6730.